Matrix formalism of electromagnetic wave propagation through multiple layers in the near-field region: Application to the flat panel display

C. Y. Lee, D. E. Lee, Y. K. Hong, J. H. Shim, C. K. Jeong, and J. Joo*
Department of Physics, Korea University, Seoul 136-701, Korea

D. S. Zang, M. G. Shim, J. J. Lee, J. K. Cha, and H. G. Yang
Samsung SDI Co., Ltd., Yongin, Kyungki-do 449-557, Korea

(Received 26 October 2001; revised manuscript received 19 November 2002; published 11 April 2003)

We have developed an electromagnetic (EM) wave propagation theory through a single layer and multiple layers in the near-field and far-field regions, and have constructed a matrix formalism in terms of the boundary conditions of the EM waves. From the shielding efficiency (SE) against EM radiation in the near-field region calculated by using the matrix formalism, we propose that the effect of multiple layers yields enhanced shielding capability compared to a single layer with the same total thickness in conducting layers as the multiple layers. We compare the intensities of an EM wave propagating through glass coated with conducting indium tin oxide (ITO) on one side and on both sides, applying it to the electromagnetic interference (EMI) shielding filter in a flat panel display such as a plasma display panel (PDP). From the measured intensities of EMI noise generated by a PDP loaded with ITO coated glass samples, the two-side coated glass shows a lower intensity of EMI noise compared to the one-side coated glass. The result confirms the enhancement of the SE due to the effect of multiple layers, as expected in the matrix formalism of EM wave propagation in the near-field region. In the far-field region, the two-side coated glass with ITO in multiple layers has a higher SE than the one-side coated glass with ITO, when the total thickness of ITO in both cases is the same.

DOI: 10.1103/PhysRevE.67.046605 PACS number(s): 41.20.Jb, 07.50.Hp, 07.07.Hj

I. INTRODUCTION

Electromagnetic (EM) wave propagation through various media with dielectric, conducting, and magnetic characteristics is well established in classical electrodynamics [1]. EM wave propagation is classified into two categories, the near-field and far-field regions, according to the ratio of the distance (r) between the radiation source and the detector to the wave number (k) of the EM waves. The EM wave propagation in the far-field region ($kr \gg 1$) had been described using plane waves for both the cases of a single layer and multiple layers in the radio, microwave, and optical frequency ranges [1]. However, EM wave propagation in the near-field region ($kr \ll 1$) has been understood for the case of a single layer only by means of the approximation of electric or magnetic dipole radiation, and is not well formulated for the case of multiple layers [1–3].

EM wave propagation includes the reflection, absorption, and transmission characteristics of medium. The transmission characteristics are related to the shielding capability against EM-radiation in the radio and microwave frequency ranges. With the rapidly increasing use of electronic products, there has been increased interest in electromagnetic interference (EMI) problems. Unexpected EM radiation generated from electronic products causes a malfunction in instrument components and degradation in the performance of devices [3–5]. As electronic products are used in closer proximity, a complete understanding of EM wave propagation in the near-field region is required. Theoretically, multiple layers with lower transmittance (i.e., better shielding capability) than a single layer with the same thickness [6–8] can be used as a shielding filter against EM radiation for flat panel displays, such as a plasma display panel (PDP) radiating a high intensity of EM waves in the radio and microwave frequency ranges.

In this report, we introduce a matrix formalism of EM wave propagation theory through a medium composed of multiple layers in the near-field as well as in the far-field region. We show the theoretical shielding efficiency (SE) equivalent to the transmittance obtained from our matrix formalism, and study the relation between the experimental SE and the EM wave intensity through the shielding filter. Finally, we discuss the effect of multiple layers yielding a higher shielding capability.

II. THEORY

The structure of the multiple layers considered is shown in Fig. 1. Assuming EM waves are normally incident on the layers, the source of the EM wave with frequency f is located at the position $x=0$, and r denotes the distance from the source to the first layer. The incident medium before the first layer and the transmitted medium after the Nth layer have conductivities σ_I and σ_T, electrical permittivities ϵ_I and ϵ_T, and magnetic permeabilities μ_I and μ_T, respectively. The jth layer with conductivity σ_j, electrical permittivity ϵ_j, magnetic permeability μ_j, and thickness d_j occupies the range $x=D_{j-1}$ to $x=D_j$, where $D_j=r+\Sigma_{l=1}^{j}d_l$ for $j>0$ and $D_0=r$. E_j (k_j) and E_{Rj} (k_{Rj}) are the electric fields (wave vectors) of the incident and reflected EM waves at $x=D_{j-1}$, respectively. E_I (k_I) and E_R (k_R) are the electric

*Author to whom correspondence should be addressed. FAX: +82-2-927-3292. Electronic address: jjoo@korea.ac.kr

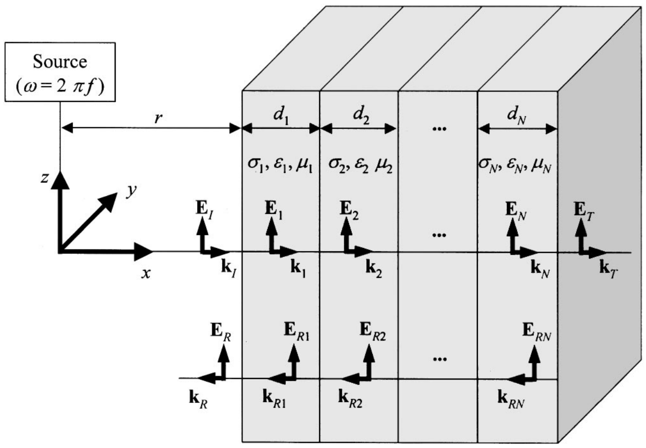

FIG. 1. Schematic structure of multiple layers. The wave vectors of the EM wave are normal to the layers, and the electric and magnetic fields are parallel to the layers and orthogonal to each other.

fields (wave vectors) of the incident and reflected EM waves at $x = D_0$, respectively, and E_T (k_T) is the electric field (wave vector) of the transmitted EM wave at $x = D_N$.

A. Near-field region

The near-field region is divided into the two subcategories, the electric field dominant and magnetic field dominant cases. When the source of the EM wave has a high voltage and a low current, the electric field from the electric dipoles is dominant. When the source of the EM wave has a low voltage and a high current, the magnetic field from the magnetic dipoles is dominant [3,5]. We assume that electric and magnetic dipoles located at the origin oscillate along the z axis with angular frequency ω and that the multiple layers are located in the yz plane as shown in Fig. 1.

1. Electric field dominant case

In the case of electric dipole radiation, the electric field E and magnetic field $H = (ik^2 r/\mu\omega)E$ in the near-field region are proportional to $1/r^3$ and $1/r^2$, respectively, and the wave impedance is given by $Z_{\mathrm{near}}^{\mathrm{elec}} = -(i/kr)Z_{\mathrm{far}}$ [1,3]. The relation between the E fields of the incident, reflected, and transmitted EM waves is obtained as

$$\begin{bmatrix} E_I \\ E_R \end{bmatrix} = \begin{bmatrix} 1 & 1 \\ \dfrac{k_I^2 D_0}{\mu_I} & -\dfrac{k_I^2 D_0}{\mu_I} \end{bmatrix}^{-1} \prod_{j=1}^{N} A_j B_j^{-1} \begin{bmatrix} 1 \\ \dfrac{k_T^2 D_N}{\mu_T} \end{bmatrix} E_T . \tag{1}$$

Here, the matrices A_j and B_j are described by

$$A_j = \begin{bmatrix} 1 & 1 \\ \dfrac{k_j^2 D_{j-1}}{\mu_j} & -\dfrac{k_j^2 D_{j-1}}{\mu_j} \end{bmatrix}$$

and

$$B_j = \begin{bmatrix} \gamma_j^3 & \gamma_j^{-3} \\ \dfrac{k_j^2 D_{j-1}}{\mu_j}\gamma_j^2 & -\dfrac{k_j^2 D_{j-1}}{\mu_j}\gamma_j^{-2} \end{bmatrix},$$

where $\gamma_j = D_{j-1}/D_j$. The complex wave vector k_j follows the dispersion relation $k_j^2 = \omega^2 \mu_j \epsilon_j + i\omega\mu_j\sigma_j$. The real and imaginary parts of k_j are given by [1]

$$\mathrm{Re}(k_j) = \omega\sqrt{\mu_j|\epsilon_j|/2}\left[\sqrt{1+(\sigma_j/\omega\epsilon_j)^2} \pm 1\right]^{1/2}, \tag{2}$$

$$\mathrm{Im}(k_j) = \omega\sqrt{\mu_j|\epsilon_j|/2}\left[\sqrt{1+(\sigma_j/\omega\epsilon_j)^2} \mp 1\right]^{1/2}. \tag{3}$$

The upper and lower signs in Eqs. (2) and (3) are applied for positive and negative ϵ_j, respectively. From Eq. (1), the reflectance $R = |E_R/E_I|^2$ and transmittance $T = |E_T/E_I|^2$ of the E field can be calculated.

2. Magnetic field dominant case

In the case of magnetic dipole radiation, the electric field E and magnetic field $H = (i/\mu\omega r)E$ in the near-field region are proportional to $1/r^2$ and $1/r^3$, respectively, and the wave impedance is given by $Z_{\mathrm{near}}^{\mathrm{mag}} = -ikrZ_{\mathrm{far}}$ [1,3]. The relation between the E fields of the incident, reflected, and transmitted EM waves can be obtained as follows:

$$\begin{bmatrix} E_I \\ E_R \end{bmatrix} = \begin{bmatrix} 1 & 1 \\ \dfrac{1}{\mu_I D_0} & -\dfrac{1}{\mu_I D_0} \end{bmatrix}^{-1} \prod_{j=1}^{N} A_j B_j^{-1} \begin{bmatrix} 1 \\ \dfrac{1}{\mu_T D_N} \end{bmatrix} E_T . \tag{4}$$

Here, the matrices A_j and B_j are described by

$$A_j = \begin{bmatrix} 1 & 1 \\ \dfrac{1}{\mu_j D_{j-1}} & -\dfrac{1}{\mu_j D_{j-1}} \end{bmatrix}$$

and

$$B_j = \begin{bmatrix} \gamma_j^2 & \gamma_j^{-2} \\ \dfrac{1}{\mu_j D_{j-1}}\gamma_j^3 & -\dfrac{1}{\mu_j D_{j-1}}\gamma_j^{-3} \end{bmatrix}.$$

From Eq. (4), the reflectance $R = |E_R/E_I|^2$ and transmittance $T = |E_T/E_I|^2$ of the E field can be directly calculated.

B. Far-field region

For the far-field region, the EM wave is described in terms of a plane wave. The electric field E and magnetic field $H = (k/\mu\omega)E$ are constant without regard to r, and the wave impedance is given by $Z_{\mathrm{far}} = E/H = \sqrt{\mu/\epsilon}$ [1,3]. Applying the boundary conditions for the E and H fields, the relation between the E fields of incident, reflected, and transmitted EM waves with respect to multiple layers is obtained as

$$\begin{bmatrix} E_I \\ E_R \end{bmatrix} = \begin{bmatrix} 1 & 1 \\ \frac{k_I}{\mu_I} & -\frac{k_I}{\mu_I} \end{bmatrix}^{-1} \prod_{j=1}^{N} A_j B_j^{-1} \begin{bmatrix} 1 \\ \frac{k_T}{\mu_T} \end{bmatrix} E_T. \quad (5)$$

Here, the matrices A_j and B_j are described by

$$A_j = \begin{bmatrix} 1 & 1 \\ \frac{k_j}{\mu_j} & -\frac{k_j}{\mu_j} \end{bmatrix}.$$

and

$$B_j = \begin{bmatrix} \exp(ik_j d_j) & \exp(-ik_j d_j) \\ \frac{k_j}{\mu_j}\exp(ik_j d_j) & -\frac{k_j}{\mu_j}\exp(-ik_j d_j) \end{bmatrix}.$$

From Eq. (5), the reflectance $R = |E_R/E_I|^2 = |H_R/H_I|^2$ and transmittance $T = |E_T/E_I|^2 = |H_T/H_I|^2$ can be directly calculated, and the SE against EM radiation is defined as [2,3,5]

$$\mathrm{SE} \equiv 20 \log_{10} |E_I/E_T| = -10 \log_{10} T. \quad (6)$$

Assuming that the media are nonmagnetic and the incident and transmitted waves are in vacuum, the SE against EM radiation through a single layer in the far-field region is described as [3]

$$\mathrm{SE} = 20 \log_{10} \left| \frac{1}{4n} [(1+n)^2 \exp(-ikd) - (1-n)^2 \exp(ikd)] \right|, \quad (7)$$

where $n = ck/\omega$ is the complex index of refraction. Equation (7) obtained by a matrix formalism based on the boundary conditions is in accordance with previously reported results derived from the transmission line formalism based on a component analysis of the contribution to the SE by reflection, absorption, and multiple reflections [9].

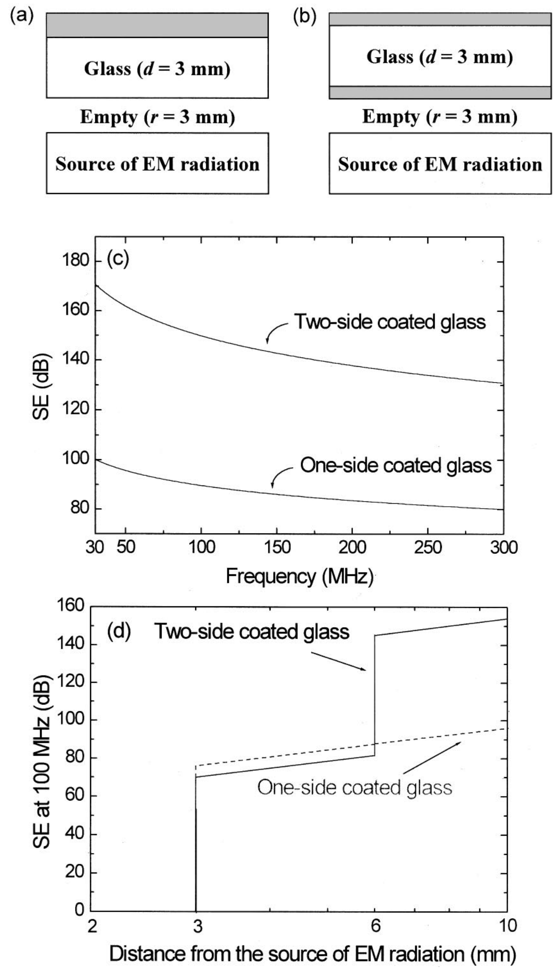

FIG. 2. Structures of (a) one-side and (b) two-side coated glass with conducting material. Relatively dark regions represent the conducting layer, such as 10 Ω ITO glass ($\sigma \simeq 7000$ S/cm). (c) Comparison of theoretical SE in the near-field region between one-side and two-side coated glasses. (d) Theoretical SEs as a function of distance from the EM radiation source for one-side and two-side coated glasses at a particular frequency ($f = 100$ MHz).

III. RESULTS AND DISCUSSION

A. Near-field region: Application to the flat panel display

1. Simulation: Electric field dominant case

In order to apply the matrix formalism, we selected glass samples coated on one side and on both sides with conducting material, such as ITO (indium tin oxide) glass with a surface resistance of 10 Ω/□ ($\sigma \simeq 7000$ S/cm, $d \simeq 1500$ Å). The two-side coated glass was intended to increase the SE by means of the effect of multiple layers. The thickness of the conducting layer on the one-side coated glass shown in Fig. 2(a) is 1500 Å. In the two-side coated glass shown in Fig. 2(b), the thickness of the first conducting layer is 750 Å, and the thickness of the second conducting layer is 750 Å. It is noted that the total thicknesses of the conducting layers with $\sigma = 7000$ S/cm are the same as 1500 Å. For a PDP as a practical example, the frequency (wavelength) range of the noise is 30–300 MHz (1–10 m). The distance between the source of the EM radiation and the conducting filter is $r = 3$ mm in vacuum, and the thickness of the glass is 3 mm, which is a typical situation for a PDP. Furthermore, the relatively high voltage required in a PDP suggests that the shielding filter against EM radiation can be treated in terms of electric dipole radiation in the near-field region ($kr \ll 1$). In Fig. 2(c), we compare the theoretical SE in the near-field region between the one-side coated glass and the two-side coated glass samples in the frequency range 30–300 MHz. In spite of having the same thicknesses, the SE of the two-side coated glass is higher than that of the one-side coated glass in the near-field region. This demonstrates our intent to increase the shielding capability by means of multiple layers as shown in Figs. 2(c) and 2(d). We propose that the conducting layers of the two-side coated glass contribute doubly to the SE predominantly due to the reflection of EM waves, and that the E field of the EM wave intrinsically decreases by $\sim 1/r^3$ for the electric field dominant case in the near-field

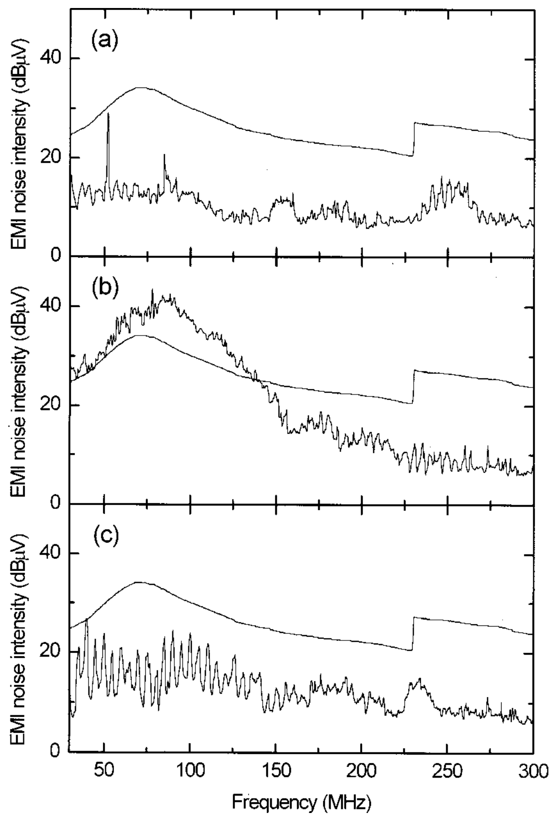

FIG. 3. Comparison of the intensity of EMI noise generated by PDP loaded with (a) commercial mesh filter, (b) one-side coated glass with 10 Ω ITO, and (c) two-side coated glass with 10 Ω ITO as a shielding filter. The solid curves are the thresholds of the EMI noise level for commercial use of PDPs.

region, as shown in Fig. 2(d). This result provides motivation for developing a shielding filter composed of multiple layers in the near-field region.

2. Experiment

For the measurements in the near-field region, the filter samples were loaded at the front side of the PDP, and EMI noise generated by the PDP was measured in a shielded room using the KEC (Kansai Electronic Industry Development Center) method. For the filter samples, the glass samples coated with conducting ITO were prepared by sputtering. The distance from the PDP to the antenna was 3 m, and the signal was detected by a Hewlett-Packard 8568B spectrum analyzer in the frequency range 30–300 MHz. The antenna was rotated 90° for the parallel and perpendicular polarizations of the EM wave. In addition, the PDP was rotated 360° to measure the maximum intensity of EM radiation emitted from the back side as well as from the front side of the PDP. The measured intensities of EMI noise generated by the PDP loaded with various shielding filter samples are compared in Fig. 3. Here, the typical measurement error of the EMI noise intensity was ± 0.5 dB μV at a single frequency. Since all the EM radiation from the PDP does not pass the shielding filter loaded at the front side, it is difficult to enumerate the EMI SE of the shielding filter from the EMI noise intensity data. For this reason, we presented the EMI noise intensity in units of dB μV as shown in Fig. 3. The solid curves in Fig. 3 represent the upper limits of the EMI noise intensities for commercial use of the filter. For a commercial mesh used in the PDP, the maximum and average intensities of EMI noise were measured to be 29.1 dB μV at 52.1 MHz and $\sim 10 \pm 3$ dB μV, respectively, as shown in Fig. 3(a). For the one-side coated glass with 10 Ω ITO, a high intensity of EMI noise was observed, and the maximum intensity was 43.4 dB μV at 78.1 MHz, which yielded an unsatisfactory result below 150 MHz, as shown in Fig. 3(b). For the two-side coated glass with 10 Ω ITO, the maximum and average intensities of EMI noise were measured to be 27.7 dB μV at 39.5 MHz and $\sim 12 \pm 4$ dB μV, respectively, as shown in Fig. 3(c). The two-side coated glass with 10 Ω ITO shows a relatively low intensity of EMI noise comparable to the commercial mesh, while the one-side coated glass fails in EMI regulation at low frequencies ($\lesssim$150 MHz). This supports the idea that the shielding capability is enhanced by multiple layers in the two-side coated glass, and demonstrates that the experimental results are qualitatively in accordance with the results of the theoretical simulation for the electric field dominant case in the near-field region.

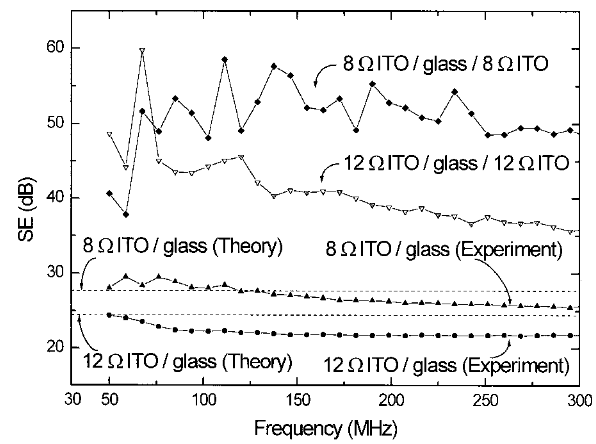

FIG. 4. Comparison of the measured SE in the far-field region between one-side and two-side coated glasses with ITO. The broken lines represent the theoretical SEs of one-side coated glasses.

B. Far-field region

In order to compare the EMI SE of the one-side and two-side coated glasses with ITO in the far-field region, we used ITO with 8 Ω/□ ($\sigma \simeq 6900$ S/cm, $d \simeq 1800$ Å) and 12 Ω/□ ($\sigma \simeq 6400$ S/cm, $d \simeq 1300$ Å). The Electro-Metrics 2107A shielding effectiveness test fixture was used. As the signal generator and EM wave receiver, a Hewlett-Packard 8719ES vector network analyzer was used. The reflected and transmitted signals were received using a built-in S (scattering) parameter set. The SE of filter samples in the far-field region was measured in the frequency range of 50 MHz–1.5 GHz using the ASTM (American Society for Testing and Materials) D4935-99 method at room temperature [10]. For measurements using the ASTM holder, the typical measurement error was ± 0.5 dB at a single frequency. The experimental SEs for the one-side and two-side coated glasses with ITO in the far-field region are compared in Fig. 4. The SEs of the 8 Ω ITO/glass and the 12 Ω ITO/glass samples are ∼27 and ∼22 dB, respectively. These results on one-side coated glasses are in relatively good agreement with the theoretical behavior in the far-field region. The SE of the 8 Ω ITO/glass/8 Ω ITO sample is ∼50 dB, while that of the 8 Ω ITO/glass sample is 25–30 dB. The total thickness of the conducting layers in the two-side coated glass is larger than in the one-side coated glass. The increase of SE by absorption due to thicker conducting layers is negligible, so that the higher SE of the two-side coated glasses is caused by the effect of multiple layers. We also observe that the SE of the 12 Ω ITO/glass/12 Ω ITO sample is higher than that of the 8 Ω ITO/glass sample, as shown in Fig. 4. Because of the poor electrical conduction caused by insulating glasses in two-side coated glasses, the experimental SE of the two-side coated glasses is higher than the theoretical SE. These results on two-side coated glasses qualitatively agree with the theoretical behavior in the far-field region described in Sec. II B.

IV. CONCLUSION

We have developed a matrix formalism of EM wave propagation theory through multiple layers in the near-field and far-field regions in terms of the boundary conditions of the EM waves. From the theoretical SE in the near-field region, we propose that the transmittance of EM radiation is significantly reduced by multiple layers. For the electric field dominant case in the near-field region, the electric field of the EM radiation rapidly decreases ($E \sim 1/r^3$) as the distance from the source of the EM wave to the boundary increases. From measurements of EMI noise generated by a PDP loaded with shielding filter samples, the two-side coated glass with 10 Ω ITO shows a low intensity of the transmitted EM wave comparable to that of the commercial mesh, which can be applied to an EMI shielding filter for a flat panel display. From measurements of SE in the far-field region, the two-side coated glass has a higher SE than the one-side coated glass. The results support the enhancement of the shielding capability with multiple layers, as proposed in the theoretical simulation using the matrix formalism of EM wave propagation theory.

ACKNOWLEDGMENTS

This study was supported in part by Samsung SDI Co. and Korea Basic Science Institute (KBSI).

[1] J. D. Jackson, *Classical Electrodynamics*, 3rd ed. (Wiley, New York, 1999).

[2] N. F. Colaneri and L. W. Shacklette, IEEE Trans. Instrum. Meas. **41**, 291 (1992).

[3] H. W. Ott, *Reduction Techniques in Electronic Systems* (Wiley, New York, 1987).

[4] R. W. Brown and S. M. Shvartsman, Phys. Rev. Lett. **83**, 1946 (1999).

[5] C. R. Paul, *Introduction to Electromagnetic Compatibility* (Wiley, New York, 1992).

[6] C. Y. Lee, H. G. Song, K. S. Jang, E. J. Oh, A. J. Epstein, and J. Joo, Synth. Met. **102**, 1346 (1999).

[7] J. Joo and C. Y. Lee, J. Appl. Phys. **88**, 513 (2000).

[8] C. Y. Lee, H. M. Kim, J. W. Park, Y. S. Gal, J. I. Jin, and J. Joo, Synth. Met. **117**, 109 (2001).

[9] R. B. Schulz, V. C. Plantz, and D. R. Brush, IEEE Trans. Comput. **EMC-30**, 187 (1988).

[10] ASTM D4935-99, *Standard Test Method for Measuring the Electromagnetic Shielding Effectiveness of Planar Materials*, 1999; Y. K. Hong, C. Y. Lee, C. K. Jeong, D. E. Lee, K. Kim, and J. Joo, Rev. Sci. Instrum. **74**, 1098 (2003).